Ion-impact ionization of He targets

M. Brauner and J. H. Macek
Department of Physics and Astronomy, University of Tennessee, Knoxville, Tennessee 37996
and Oak Ridge National Laboratory, Oak Ridge, Tennessee 37831
(Received 8 April 1992)

We calculate double-differential cross sections for the impact ionization of He targets by 1.5-MeV H^+ and 28.5-MeV F^{9+} ions using the distorted-wave strong-potential Born approximation. The theory is compared with the experimental electron spectrum. Both theory and experiment show the low-energy electron distribution, the electron capture to the continuum cusp, and the binary-encounter peak.

PACS number(s): 34.50.Fa

I. INTRODUCTION

The energy and angular distribution of electrons ejected from atoms by ion impact [doubly differential cross sections (DDCS)] have long been used to probe ionization mechanism in ion-atom collisions [1,2]. Some of these mechanisms, for example, autoionization, explicitly involve multielectron interactions but important single-electron mechanisms have also emerged. The simplest mechanism is the direct ejection of an atomic electron by a binary projectile-electron collision. This mechanism is characterized by a vanishing value for the momentum and energy of the recoiling target ion in the final state. When the recoil momentum vanishes, the DDCS for the ejected electron shows a peak, called the binary-encounter (BE) peak, at a specific electron momentum and energy. Because the electron is initially bound, this peak is broadened by the Compton profile of the initial state, but the details of target dynamics play no essential role. This BE peak is readily identified and compared with standard direction ionization theory.

A second mechanism, direct ejection of slow electrons, is also well studied [3]. Here the field of the fast charged particle at impact parameters outside of the range of the initial $1s$ wave function perturbs the atom so that in the final state the atom is excited or ionized. Here the low-energy electron spectrum is seen as a continuation of excitation across the ionization threshold. For initial $1s$ states the ejected electron spectrum in the low-energy region decreases monotonically from a maximum value at zero energy. The corresponding zero-energy peak is well understood in terms of the first Born theory for direct ionization [4] (DI).

The two peaks just mentioned have long been understood for fast ions of low charge. In contrast, a third peak due to the capture of electrons to continuum state (ECC) mechanisms was identified much later [5–7]. This mechanism is characterized by a cusp at an electron velocity which matches the ion velocity in the final state. Because the cusp represents a rearrangement process, the theory of this effect requires a higher-order approximation for the amplitude. Initial computations employing the lowest-order Brinkman-Kramers amplitude are quantitatively inaccurate [7] and a higher-order theory must be used [8].

The three mechanisms, binary encounter, direct ejection of slow electrons, and continuum electron capture, are known experimentally even for collisions involving highly charged ions. In this case, as emphasized by Briggs [9] in connection with electron capture, it is natural to employ an expansion in powers of the smaller charge of target Z_T rather than the charge of the projectile Z_P as done in standard first Born theories of ionization. Then one obtains quite naturally the distorted-wave strong-potential Born theory (DSPB) of ionization by highly charged ions. With the formulation given by Macek [10] expansions in powers of charge are free of divergences noted by Dewangan and Eichler [11]. Our objective in this paper is to apply the DSPB theory of Taulbjerg, Barrachina, and Macek [12] to the ionization of He by 1.5 MeV/amu H^+ and F^{9+} impact, where measurements are available [13].

It is clear that the DSPB theory includes the ECC cusp, but it is less clear that the binary-encounter peak and the slow electrons are well described in this theory. For that reason we compute the DDCS for electrons ejected at 0° and electron energies which include the slow electrons, cusp electrons, and binary-encounter electrons. The notation is described in Sec. II and the general theory in Sec. III. Results are discussed in Sec. IV and Sec. V presents some concluding remarks.

For more asymmetric collision systems Jakubassa-Amundsen [14] uses the semiclassical impulse approximation (SCIA) and a peaking approximation to evaluate the SCIA matrix element. This theory is similar to the present DSPB theory. It uses a more restrictive peaking approximation than is used in our DSPB calculations, but less restrictive than used in the peaked-DSPB calculations.

Three other higher-order theories, namely, the exact impulse approximation (IA) of Miraglia and Macek [15], the continuum-distorted-wave (CDW-CDW) calculations of Belkic [16], and the continuum-distorted-wave–eikonal-initial-state (CDW-EIS) theory of Fainstein, Ponce, and Rivarola [17], have been used to compute ejected electron spectra for highly charged ions. We show that these theories are all very similar and give ionization amplitudes which are quite similar in form.

There are important differences, however, in that the CDW-CDW amplitude diverges while the CDW-EIS amplitude lacks the Thomas peak. The IA amplitude of Miraglia and Macek [15] is convergent everywhere and includes the Thomas peak. This theory differs from the present theory in that our DSPB theory is much less computer intensive. In addition, a peaked form of the DSPB amplitude (PDSPB) is available which is readily compared with other theories. The CDW-CDW theory is described in Appendix C for comparison with the DSPB amplitude, but because it is divergent no numerical results are given here. The form of the CDW-EIS amplitude is also compared with our peaked DSPB amplitude in Sec. III. The reader is referred to the paper of Crothers and McCann [18] for quantitative calculations using the CDW-EIS theory.

Our quantitative calculations employ the model of Bates and Griffing for the two-electron helium atom. Because this model was initially employed only for first Born calculations of direct ionization we show that the model derives generally from the independent-particle approximation with specific choices for independent-particle wave functions. The form used in the present work employs further approximation described in Appendix B.

II. NOTATION

We consider ionization of a neutral atom (T,e) composed of a nucleus T and an electron e by impact of a projectile P;

$$P+(T,e)\rightarrow P+T+e \ . \tag{1}$$

Charges of the projectile and target nuclei are Z_P and Z_T, respectively. Let $\mathbf{r}_P$ and $\mathbf{r}_T$ represent the position of the electron with respect to P and T, respectively. The position of the center of mass of the system (P,e) relative to T is $\mathbf{R}_P$ and $\mathbf{R}_T$ describes the position of P relative to the center of mass of (T,e) (Fig. 1). After the scattering the momenta corresponding to $\mathbf{r}_P$, $\mathbf{r}_T$, $\mathbf{R}_P$, and $\mathbf{R}_T$ are $\mathbf{k}_P$, $\mathbf{k}_T$, $\mathbf{K}_P$, and $\mathbf{K}_T$. The masses of projectile, nucleus, and electron are M_P, M_T, and m. Atomic units are used throughout this work but m is retained in some equations for clarity.

The momentum transfer vectors $\mathbf{K}$ and $\mathbf{J}$ of Shakeshaft [19] are employed. They are defined as

$$\mathbf{K}=\beta\mathbf{K}_f-\mathbf{K}_i \ , \tag{2}$$

$$\mathbf{J}=\alpha\mathbf{K}_i-\mathbf{K}_f \ , \tag{3}$$

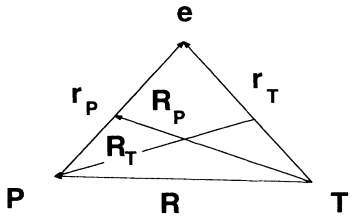

FIG. 1. The set of Jacobi coordinates.

with

$$\alpha=M_T/(M_T+m); \quad \beta=M_P/(M_P+m) \ , \tag{4}$$

$\mathbf{K}_i$ is the relative momentum of P and (T,e) before the scattering, and $\mathbf{K}_f=\mathbf{K}_P$. The total energy E is expressed as

$$E=E_i=E_f \ , \tag{5}$$

$$E_i=\frac{K_i^2}{2\mu_{P,Te}}+\varepsilon_i \ , \tag{6}$$

$$E_f=\frac{K_f^2}{2\mu_{T,Pe}}+\frac{k_P^2}{2\mu_{Pe}}=\frac{K_f^2}{2\mu_{T,Pe}}+\varepsilon_f \ , \tag{7}$$

where ε_i is the binding energy (T,e) in the initial state and the reduced masses

$$\mu_{i,kl}=\frac{M_i(M_k+M_l)}{M_i+M_k+M_l}, \quad \mu_{kl}=\frac{M_kM_l}{M_k+M_l} \tag{8}$$

are employed. The velocity vector $\mathbf{v}$ is defined according to

$$\mathbf{v}=\frac{\mathbf{K}_i}{\mu_{P,Te}} \ . \tag{9}$$

To order $O(m/M_T, m/M_p)$ we have

$$\mathbf{K}+\mathbf{J}+m\mathbf{v}=\mathbf{0} \tag{10}$$

and

$$K^2+2\varepsilon_i=J^2+2\varepsilon_f \ . \tag{11}$$

The differential cross section is given by

$$\frac{d\sigma}{d\mathbf{k}_P}=(2\pi)^4\int\frac{\mu_{P,Te}}{K_i}|T|^2\delta(E_f-E_i)d\mathbf{K}_P \ , \tag{12}$$

which can be transformed into an integral over the momentum transfer $K=|\mathbf{K}|$.

$$\frac{d\sigma}{dE_e d\Omega_e}=\frac{(2\pi)^4}{v^2}k_T\int_{K_{\min}}^{\infty}dK\,K\int_0^{2\pi}d\varphi_K|T|^2 \ , \tag{13}$$

with

$$K_{\min}=\frac{v^2+Z_T^2+k_P^2}{2v} \ . \tag{14}$$

Here $d\Omega_e$ and E_e are the solid angle and energy of the ionized electron in the target frame and $d\varphi_K$ is the azimuthal angle of $\mathbf{K}$ relative to a plane. For electrons ejected in the forward direction $|T|^2$ is independent of φ_K and we use

$$\frac{d\sigma}{dE_e d\Omega_e}=\frac{(2\pi)^5}{v^2}k_T\int_{K_{\min}}^{\infty}dK\,K|T|^2 \ . \tag{15}$$

In general the T matrix is written as (postform)

$$T=\langle\Phi_f^{(-)}|V_f-U_f|\Psi_i^{(+)}\rangle \tag{16}$$

$$=\langle\Phi_f^{(-)}|(V_f-U_f)[1+G(V_i-U_i)]|\Phi_i^{(+)}\rangle \ , \tag{17}$$

where G is the full Green's operator, V_i (V_f) the poten-

tial in the initial (final) channel, and U_i (U_f) are distortion potentials used to compute $\Phi_{i,f}^{(\pm)}$. These later potentials are chosen so that V_f-U_f and V_i-U_i vanish faster than $1/R$ as $R\to\infty$, but are otherwise arbitrary. They ensure that all integrals in the definition T are well defined.

III. THEORY

A. The DSPB theory for ionization

Briggs [9] has emphasized the utility of expansions of T in powers of Z_T. This expansion has been developed further by many workers [20–23]. Following Taulbjerg, Barrachina, and Macek [12] we expand Eq. (17) in powers of Z_T to obtain the distorted-wave strong-potential Born amplitude

$$T^{\mathrm{DSPB}}=\langle\Phi_f|(V_T-U_T)|\Phi_i^{\mathrm{DSPB}(+)}\rangle + Z_T\langle\Phi_f^{1(-)}|V_T|\Phi_i^{(+)}\rangle \ , \tag{18}$$

where Φ_f and $\Phi_f^{1(-)}$ are the zeroth- and first-order terms in the expansion of $\Phi_f^{(-)}$ in powers of Z_T and $\Phi_i^{\mathrm{DSPB}(+)}$ is given by

$$|\Phi_i^{\mathrm{DSPB}(+)}\rangle=G_P V_T|\Phi_i^{(+)}\rangle \ , \tag{19}$$

with

$$V_T=-\frac{Z_T}{r_T} \ , \tag{20}$$

$$V_P=-\frac{Z_P}{r_P} \ . \tag{21}$$

The potential $U_T(\mathbf{R}_T)$ goes to $-Z_T/R_T$ as $R_T\to\infty$ but is otherwise arbitrary. Note that the strong potential V_P ($Z_P\gg Z_T$) is retained to all orders in the Coulomb Green function G_P.

The initial state Φ_i is the product of a hydrogenic $1s$ state and a plane wave describing the motion of the projectile,

$$\Phi_i=(2\pi)^{-3/2}e^{i\mathbf{K}_i\cdot\mathbf{R}_T}\varphi_{1s}(\mathbf{r}_T) \ , \tag{22}$$

$$\varphi_{1s}(\mathbf{r}_T)=\left[\frac{Z_T^3}{\pi}\right]^{1/2}e^{-Z_T r_T} \ . \tag{23}$$

For ionization of two-electron helium atoms we use the Bates-Griffing independent-electron model [24] which employs $Z_T=(-2\varepsilon_i)^{1/2}=1.345$. Since this model was initially proposed for first-order Born amplitudes and its extension to higher-order theories is not obvious, we discuss the justification of this model for highly charged ions in Appendix B.

The final-state wave function Φ_f is the production of a plane wave of relative motion and a Coulomb wave of the projectile-electron system;

$$\Phi_f=(2\pi)^{-3/2}e^{i\mathbf{K}_f\cdot\mathbf{R}_P}\psi_{\mathbf{k}_P}^{(-)}(\mathbf{r}_p) \ , \tag{24}$$

$$\psi_{\mathbf{k}_P}^{(-)}(\mathbf{r}_P)=(2\pi)^{-3/2}e^{\pi\beta_P/2}\Gamma(1+i\beta_P)e^{i\mathbf{k}_P\cdot\mathbf{r}_P} \times{}_1F_1(-i\beta_P;1;-i[k_P r_P+\mathbf{k}_P\cdot\mathbf{r}_P]) \ , \tag{25}$$

with the Sommerfeld parameter

$$\beta_P=\frac{Z_P}{k_P} \ . \tag{26}$$

An approximate DSPB amplitude derives from Eq. (18) using several peaking approximations [12]. We use

$$T^{\mathrm{DSPB}(+)}=(2\pi)^{-3/2}\times\int d\mathbf{s}\langle\psi_{\mathbf{k}_P}^{(-)}(\mathbf{r}_p)|e^{-i(\mathbf{J}+\mathbf{s})\cdot\mathbf{r}_P}|\Psi_{\mathbf{s}-\mathbf{v}}^{(+)}(\mathbf{r}_p)\rangle \times\tilde{V}_T(\mathbf{s}+\mathbf{J})\tilde{\varphi}_{1s}(\mathbf{s})\gamma(\mathbf{s}) \ , \tag{27}$$

where $\gamma(\mathbf{s})$ is a modified off-shell factor given by Taulbjerg, Barrachina, and Macek [12], $\tilde{\varphi}_{1s}(\mathbf{s})$ is the Fourier transform of φ_{1s}, $\psi_{\mathbf{s}-\mathbf{v}}^{(+)}$ is the Coulomb wave function

$$\psi_{\mathbf{s}-\mathbf{v}}^{(+)}(\mathbf{r}_P)=(2\pi)^{-3/2}e^{+\pi\nu_P/2}\Gamma(1-i\nu_P)e^{i(\mathbf{s}-\mathbf{v})\cdot\mathbf{r}_P} \times{}_1F_1(i\nu_P;1;i[|\mathbf{s}-\mathbf{v}|r_P-(\mathbf{s}-\mathbf{v})\cdot\mathbf{r}_P]) \ , \tag{28}$$

with the Sommerfeld parameter

$$\nu_P=\frac{Z_P}{v} \ , \tag{29}$$

and $\tilde{V}_T$ is the fourier transform of V_T. We also set $\gamma(\mathbf{s})=1$. With this approximation the DSPB amplitude equals the IA amplitude of Briggs [9]. Equation (27) is then written in the momentum representation for the initial state,

$$T^{\mathrm{DSPB}(+)}=-\frac{4\pi}{(2\pi)^3}Z_T\int\frac{d\mathbf{s}}{|\mathbf{J}+\mathbf{s}|^2}\langle\psi_{\mathbf{k}_P}^{(-)}(\mathbf{r}_P)|e^{-i(\mathbf{J}+\mathbf{s})\cdot\mathbf{r}_P}|\psi_{\mathbf{s}-\mathbf{v}}^{(+)}(\mathbf{r}_P)\rangle\tilde{\varphi}_{1s}(\mathbf{s}) \ . \tag{30}$$

This expression is very similar to the semiclassical impulse approximation used by Jakubassa-Amundsen [14]. We write

$$\frac{\tilde{\varphi}_i(\mathbf{s})}{|\mathbf{J}+\mathbf{s}|^2}=-\frac{2^{3/2}Z_T^{5/2}}{\pi}\lim_{\lambda_T\to Z_T}\frac{1}{2\lambda_T}\frac{\partial}{\partial\lambda T}\frac{1}{(\mathbf{J}+\mathbf{s})^2(s^2+\lambda_T^2)} \tag{31}$$

and use the Feynman integral [25]

$$\frac{1}{ab}=\int_0^1\frac{dt}{[at+b(1-t)]^2} \tag{32}$$

to obtain

$$T^{\mathrm{DSPB}(+)}=\frac{Z_T^{5/2}}{(2\pi)^2}\lim_{\lambda_T\to Z_T}\frac{\partial}{\partial\lambda_T}\int_0^1\frac{dt}{\mu^{5/2}}\int d\mathbf{s}\langle\psi_{\mathbf{k}P}^{(-)}(\mathbf{r}_P)|e^{-i(\mathbf{J}_t+\mathbf{s})\cdot\mathbf{r}_P}|\psi_{\mathbf{s}-\mathbf{v}_t}^{(+)}(\mathbf{r}_P)\rangle\tilde{\varphi}_{1s}(\mathbf{s},\mu) \ , \tag{33}$$

with

$$\mu^2=(\lambda_T^2+J^2t)(1-t)\ , \tag{34}$$

$$\mathbf{J}_t=\mathbf{J}-\mathbf{J}t\ , \tag{35}$$

$$\mathbf{v}_t=\mathbf{v}+\mathbf{J}t\ . \tag{36}$$

Here $\tilde{\varphi}_i(\mathbf{s},\mu)$ is the Fourier transform of a hydrogenic $1s$ wave function for nuclear charge μ.

The matrix element

$$M=\langle \psi_{\mathbf{k}_P}^{(-)}(\mathbf{r}_P)|e^{-i(\mathbf{J}_t+\mathbf{s})\cdot\mathbf{r}_P}|\psi_{\mathbf{s}-\mathbf{v}_t}^{(+)}(\mathbf{r}_P)\rangle \tag{37}$$

is recognized as a Nordsieck integral with the expression [26]

$$M=-(2\pi)^{-3}N(\nu_P)N(\beta_P)\lim_{\lambda_0\to 0}\frac{\partial}{\partial\lambda_0}4\pi\frac{C^{i\nu_P+i\beta_P-1}}{A^{i\beta_P}B^{i\nu_P}} \times {}_2F_1(i\nu_P,i\beta_P;1;z)\ , \tag{38}$$

where

$$N(\alpha)=e^{\pi\alpha/2}\Gamma(1-i\alpha)\ , \tag{39}$$

$$A=(\lambda_0-ik_P)^2+K^2\ , \tag{40}$$

$$B(\mathbf{s})=\lambda_0^2-2i\lambda_0|\mathbf{s}-\mathbf{v}_t|+(\mathbf{J}_t+\mathbf{k}_P)^2 -v_t^2-2(\mathbf{K}-\mathbf{k}_P)\cdot\mathbf{s}\ , \tag{41}$$

$$C=\lambda_0^2+(\mathbf{K}-\mathbf{k}_P)^2\ , \tag{42}$$

$$D(\mathbf{s})=(\lambda_0-ik_P)^2-2(i\lambda_0+k_P)|\mathbf{s}-\mathbf{v}_t| +J_t^2-v_t^2-2\mathbf{K}\cdot\mathbf{s}\ , \tag{43}$$

$$z=1-\frac{CD}{AB}\ . \tag{44}$$

Equation (33) involves a four-dimensional integral, but with fairly weak approximations the integral over s may be done in closed form. Details are given in Appendix A.

Substituting Eq. (A27) into Eq. (33) using Eq. (31) gives

$$T^{\mathrm{DSPB}(+)}=-\frac{Z_T^{5/2}}{2^{3/2}\pi^3}N(\nu_P)N(\beta_P)\lim_{\lambda_0\to 0}\lim_{\lambda_T\to Z_T}\frac{\partial^2}{\partial\lambda_T\partial\lambda_0} \times\int_0^1\frac{dt}{\mu}\frac{C^{i\nu_P+i\beta_P-1}}{A^{i\beta_P}B^{i\nu_P}}{}_2F_1(i\nu_P,i\beta_P;1;z)\ , \tag{45}$$

where A and C are given above but B and D now no longer depend upon s;

$$B=(\lambda_0-iv_t)^2+(\mathbf{J}_t+\mathbf{k}_p)^2-2i\mu|i\lambda_0\hat{\mathbf{v}}_t+\mathbf{k}_P-\mathbf{K}|\ , \tag{46}$$

$$D=B-2k_P\left[i\lambda_0+k_P+v_t+\hat{\mathbf{k}}_P\cdot\mathbf{J}_t +i\mu\frac{i\lambda_0\hat{\mathbf{v}}_t+\mathbf{k}_P-\mathbf{K}}{|i\lambda_0\hat{\mathbf{v}}_t+\mathbf{k}_P-\mathbf{K}|}(\hat{\mathbf{v}}_t-\hat{\mathbf{k}}_P)\right]\ . \tag{47}$$

Equation (45) requires a single numerical integral and its form is thus difficult to compare with closed-form expressions of other theories such as the CDW and Born approximations. For J large compared with Z_T we may employ the peaked-DSPB approximation which takes

$$\frac{1}{|\mathbf{J}+\mathbf{s}|^2}\simeq\frac{1}{J^2+Z_T^2}\ . \tag{48}$$

It is easy to show that now the T matrix is given by

$$T^{\mathrm{PDSPB}}=\frac{Z_T^{5/2}}{\sqrt{2}\pi^3}\frac{N(\nu_P)N(\beta_P)}{J^2+Z_T^2}\lim_{\lambda_0\to 0}\frac{\partial}{\partial\lambda_0}\frac{C'^{i\nu_P+i\beta_P-1}}{A'^{i\beta_P}B'^{i\nu_P}} \times{}_2F_1(i\nu_P,i\beta_P;1;z')\ , \tag{49}$$

where

$$A'=(\lambda_0-ik_P)^2+K^2\ , \tag{50}$$

$$B'=(\lambda_0-iv)^2+(\mathbf{J}+\mathbf{k}_P)^2-2iZ_T|i\lambda_0\hat{\mathbf{v}}+\mathbf{k}_P-\mathbf{K}|\ , \tag{51}$$

$$C'=\lambda_0^2+(\mathbf{K}-\mathbf{k}_P)^2\ , \tag{52}$$

$$D'=B'-2k_P\left[i\lambda_0+k_P+v+\hat{\mathbf{k}}_P\cdot\mathbf{J} +iZ_T\frac{i\lambda_0\hat{\mathbf{v}}+\mathbf{k}_P-\mathbf{K}}{|i\lambda_0\hat{\mathbf{v}}+\mathbf{k}_P-\mathbf{K}|}(\hat{\mathbf{v}}-\hat{\mathbf{k}}_P)\right]\ , \tag{53}$$

$$z'=1-\frac{C'D'}{A'B'}\ . \tag{54}$$

This closed form expression is compared with the CDW-CDW amplitude in Sec. III B.

Near the binary-encounter peak where $k_P\simeq v$, we must have $J\simeq 0$ and $\mathbf{K}\simeq-\mathbf{v}$. Then the argument z' of the hypergeometric function in Eq. (49) is much larger than unity and an asymptotic form [see Eq. (C22)] can be used. Upon taking the derivative with respect to λ_0 and retaining only terms of lowest order in Z_T/v we have

$$T^{\mathrm{PDSPB}}\simeq -Z_P\frac{(2Z_T^5)^{1/2}}{\pi^3}\frac{1}{[J^2+Z_T^2]^2}\frac{1}{|\mathbf{K}-\mathbf{k}_P|^2} \times\left[\frac{(k_P+v)^2}{|\mathbf{K}-\mathbf{k}_P|^2}\right]^{-i\beta_P}\frac{\Gamma(1-i\nu_P)}{\Gamma(1+i\nu_P)} =T^{(\mathrm{Ruth})}(\mathbf{k}_P,\mathbf{K})\tilde{\varphi}_{1s}(-\mathbf{J})\ , \tag{55}$$

where $T^{(\mathrm{Ruth})}(\mathbf{k}_P,\mathbf{K})$ is the Rutherford scattering amplitude for the collision of an electron of momentum $\mathbf{K}\simeq-\mathbf{v}$ with a nucleus of charge Z_P. This shows that the DSPB amplitude approaches the intuitive binary collision model near the binary-encounter peak, as one would expect from a correct theory for sufficiently high v. Note here that the DSPB amplitude approaches the binary-encounter amplitude when $Z_T/v\ll 1$. In contrast the Brinkman-Kramers amplitude, discussed below, approaches the binary collision model only when $Z_P/v\ll 1$, a much more restrictive condition.

In this paper we compute cross sections for electrons ejected in the forward direction using Eqs. (45) and (13) multiplied by a factor of 2 (see Appendix B) to account for the two electrons on He. These cross sections are compared with the data of Lee *et al.* [13].

B. Other theories

At high velocities the Coulomb wave $\psi^{(+)}_{s-v}(\mathbf{r}_P)$ approaches a plane wave $\phi_{s-v}(\mathbf{r}_P)$. When $\psi^{(+)}_{s-p}(\mathbf{r}_P)$ is replaced by $\phi_{s-v}(\mathbf{r}_P)$ the DSPB amplitude becomes the first-order Brinkman-Kramers amplitude for electron capture to the continuum. Note that this way of deriving the first-order amplitude omits the potential U_T as correctly surmised by Brinkman and Kramers [4,27] and by later authors. The omission of U_T occurs naturally here owing to effects of higher-order terms in Z_P, i.e., $\psi^{(+)}_{s-v}$ is orthogonal to $\psi^{(+)}_{\mathbf{k}_P}$ but $\phi_{s-v}(\mathbf{r}_P)$ is not. Standard derivations omit U_T at the outset thus the omission of U_T has been controversial. Here we have shown that such omission derives from first principles.

The electron capture to the continuum amplitude in the Brinkman-Kramers approximation is

$$T^{\mathrm{ECC}}=\langle \psi^{-}_{\mathbf{k}_p}|V_P|\phi_{\mathbf{K}}\rangle \tilde{\varphi}_{1s}(-\mathbf{J}) \ . \tag{56}$$

Superficially, this expression appears to agree with the intuitive binary-encounter model, since the matrix element $\langle \psi^{-}_{\mathbf{k}_p}|V_P|\phi_{\mathbf{K}}\rangle$ is often replaced by the Rutherford scattering amplitude [4]. This replacement is incorrect and direct evaluation of the matrix element yields

$$T^{\mathrm{ECC}}=-Z_P\frac{(2Z_T^5)^{1/2}}{\pi^3}\frac{1}{[J^2+Z_T^2]^2}\frac{N(\beta p)}{(\mathbf{K}-\mathbf{k}_P)^2} \times\left[\frac{K^2-k_P^2}{(\mathbf{K}-\mathbf{k}_P)^2}\right]^{-i\beta_P} , \tag{57}$$

which includes the additional factor

$$e^{\pi\beta_P/2}\Gamma(1+i\beta_P)\left[\frac{K^2-k_P^2}{4k_P^2}\right]^{-i\beta_P} .$$

This factor is recognized as the off-shell factor of Taulbjerg, Barrachina, and Macek [12] and cannot simply be omitted as in some derivations (Mott and Massey [4], p. 338) since then the ECC cusp is not represented. We retain the form Eq. (57) in our calculations.

The standard first Born approximation for direct ionization uses a target Coulomb eigenstate as a final state. Since this a standard approximation widely employed in theories of charged particle interactions with matter, we compare our calculations with the Born approximation for DI. The first Born approximation for DI of one-electron ions [28] is well known. When written in terms of the momentum transfer vectors $\mathbf{J}$ and $\mathbf{K}$ we have

$$\begin{aligned}T^{\mathrm{DI}}&=\langle\Phi_f|V_P|\Phi_i\rangle\\ &=-Z_P\frac{(2Z_T)^{3/2}}{2\pi^3}\frac{e^{\pi\nu_T/2}(1-i\nu_T)}{[J^2+Z_T^2]^2|\mathbf{K}-\mathbf{k}_P|^2}\left[\frac{(\mathbf{J}+\mathbf{k}_T)^2+(Z_T-ik_T)^2}{J^2+Z_T^2}\right]^{-i\nu_T}\\ &\times\frac{Z_T(1-i\nu_T)[(\mathbf{J}+\mathbf{k}_T)^2+(Z_T-ik_T)^2]+\nu_T(k_T+iZ_T)[J^2+Z_T^2]}{(\mathbf{J}+\mathbf{k}_T)^2(Z_T-ik_T)^2} ,\end{aligned} \tag{58}$$

where

$$\nu_T=\frac{Z_T}{k_T} . \tag{59}$$

Introducing the momentum vector $\mathbf{q}$,

$$\mathbf{q}=\mathbf{K}-\mathbf{k}p=-(\mathbf{J}+\mathbf{k}_T) \tag{60}$$

give the standard expression [4]

$$\begin{aligned}|T^{\mathrm{DI}}|^2=&\frac{2}{\pi^3}\frac{Z_p^2}{q^4}\frac{Z_T}{k_T}\frac{\exp\{-(2Z_T/k_T)\tan^{-1}[2Z_Tk_T/(q^2-k_T^2+Z_T^2)]\}}{[1-\exp(-2\pi Z_T/k_T)][(q^2-k_T^2+Z_T^2)^2+(2Z_Tk_T)^2]}\\ &\times\left[(q^2+\mathbf{q}\cdot\mathbf{k}_T)^2+\left[\frac{Z_T^2}{k_T^2}\right](\mathbf{q}\cdot\mathbf{k}_T)^2\right]|\tilde{\varphi}_{1s}(\mathbf{q}+\mathbf{k}_T)|^2 .\end{aligned} \tag{61}$$

Near the binary-encounter peak we have $Z_T/k_T\ll 1$ and $\mathbf{q}=\mathbf{K}-\mathbf{k}_P\simeq-\mathbf{k}_T$ and Eq. (61) becomes

$$\begin{aligned}|T^{\mathrm{DI}}|^2&\simeq\frac{Z_P^2}{4\pi^4}\frac{1}{|\mathbf{K}-\mathbf{k}_P|^4}|\tilde{\varphi}_{1s}(-\mathbf{J})|^2\\ &=|T^{(\mathrm{Ruth})}(\mathbf{k}_P,\mathbf{K})|^2|\tilde{\varphi}_{1s}(-\mathbf{J})|^2 .\end{aligned} \tag{62}$$

This expression agrees with the intuitive binary-encounter model. It must be emphasized that only the magnitude agrees, whereas for the PDSPB amplitude both amplitude and phase agree with the intuitive model.

Belkic [16] employed the CDW-CDW theory for ionization of atomic targets by ion impact. He gives

$$T^{\mathrm{CDW-CDW}}=\langle\xi_f|-\nabla_{\mathbf{r}_P}\cdot\nabla_{\mathbf{r}_T}|\xi_i\rangle , \tag{63}$$

$$\xi_i=\Phi_iN(\nu_P)\,{}_1F_1(i\nu_P;1;i[vr_P+\mathbf{v}\cdot\mathbf{r}_P]) , \tag{64}$$

$$\xi_f=\Phi_fN(\nu_T)^*\,{}_1F_1(-i\nu_T;1;-i[vr_T+\mathbf{v}\cdot\mathbf{r}_T]) , \tag{65}$$

where Φ_i and Φ_f are given by Eqs. (22) and (24), respec-

tively. This T-matrix element is convergent and well defined for bound-state capture, where it has been extensively used, but for ionization (and excitation) the phase of the matrix element diverges [29] for particular values of $\mathbf{k}_P$ and $\mathbf{J}$. In some cases the magnitude also diverges. Since a valid expression for the scattering amplitude must converge in phase as well as magnitude [30] the CDW-CDW theory is not applicable for ionization. These divergencies are described in Appendix C.

Crothers and McCann [18] developed a continuum-distorted-wave–eikonal-initial-state theory. Here the final state is chosen as in the CDW-CDW theory whereas the hypergeometric function (64) in the initial state is replaced by its asymptotic value. As discussed in Appendix C the CDW-EIS theory is free of the divergences characteristic of the CDW-CDW theory.

The three approximations for the T-matrix element, namely, the CDW-CDW, CDW-EIS, and PDSPB, are quite similar in form since the amplitudes can be written in terms of identical hypergeometric functions; compare Eqs. (49) and (C4), for example. The main differences between them are the expressions for the argument z of the hypegeometric functions

$$z^{\text{CDW-CDW}}=\frac{\beta\gamma-\alpha\delta}{\gamma(\alpha+\beta)} , \tag{66}$$

$$z^{\text{CDW-EIS}}=\frac{\beta\gamma-\alpha\delta}{\gamma\beta} , \tag{67}$$

$$z^{\text{PDSPB}}=\frac{A'B'-C'D'}{A'B'} , \tag{68}$$

where

$$\alpha=\frac{q^2}{2} , \tag{69}$$

$$\beta=-\tfrac{1}{2}(k_T^2+Z_T^2) , \tag{70}$$

$$\gamma=\tfrac{1}{2}[(\mathbf{q}+\mathbf{k}_T)^2+Z_T^2]=\tfrac{1}{2}[J^2+Z_T^2] , \tag{71}$$

$$\delta=\mathbf{k}_P\cdot\mathbf{v}-k_P v+\beta . \tag{72}$$

The divergencies of the CDW-CDW theory occur when the factor

$$\alpha+\beta=\tfrac{1}{2}[K^2-v^2+2\mathbf{k}_P\cdot\mathbf{J}-Z_T^2]=\tfrac{1}{2}[(\mathbf{J}+\mathbf{k}_P)^2-v^2] \tag{73}$$

in the denominator of Eq. (66) vanishes. Because the corresponding factor of the CDW-EIS theory, Eq. (67),

$$\beta=\tfrac{1}{2}[-v^2-k_P^2-2\mathbf{k}_P\cdot\mathbf{v}-Z_T^2]<0 \tag{74}$$

never vanishes, the CDW-EIS theory is free of divergent terms, but since β is independent of K the CDW-EIS theory does not describe the Thomas double-collision peak [31]. For comparison the factor in the denominator of the peaked DSPB theory,

$$B'=(\mathbf{J}+\mathbf{k}_p)^2-v^2-2iZ_T|\mathbf{k}_P-\mathbf{K}| , \tag{75}$$

also never vanishes, although it becomes small near the Thomas double-collision peak. Only the DSPB amplitude in both finite everywhere and shows the Thomas peak. While the presence of the Thomas peak is important conceptually it is not great practical importance for highly charged ions. Thus we will see that the DSPB and the CDW-EIS theories agree moderately well.

The main difference of PDSPB theory and the CDW-CDW theory is the appearance of the terms with the factors iZ_T in B' and D' [Eqs. (51) and (53)]. These imaginary terms prevent the PDSPB theory from diverging. If we neglect these terms we are able to write

$$A'\simeq 2\gamma , \tag{76}$$

$$B'\simeq 2(\alpha+\beta) , \tag{77}$$

$$C'\simeq 2\alpha , \tag{78}$$

$$D'\simeq 2(\beta+\gamma) . \tag{79}$$

With this approximation it is easy to see that the variable z of the CDW-CDW theory [Eq. (66)] and the PDSPB theory [Eq. (68)] are identical for

$$\mathbf{k}_P\cdot\mathbf{v}-k_P v=0 . \tag{80}$$

This is the case in the forward direction or in any direction at the ECC cusp ($k_p=0$). Also when terms of order v_T are neglected and Eq. (80) holds then the PDSPB and CDW-CDW are identical. This shows the close relation between CDW-CDW and PDSPB. The main difference between the approximations is that the CDW neglects $2iZ_T v$ compared with $\alpha+\beta$. This latter approximation is invalid when $\alpha+\beta$ vanishes.

IV. RESULTS

Lee *et al.* [13] measured the electron spectra in the forward direction ejected by 1.5 MeV/amu H^+ and F^{9+} impact. The experimental results for H^+ and F^{9+} are compared with standard DI in Figs. 2(a) and 2(b), respectively. The experimental electron spectra show an enhancement of the cross section at low electron energies, the ECC cusp at $k_T=v$, and the binary-encounter peak at $k_T=2v$. The DI theory agrees with experiment only near the binary-encounter peak. It lacks the ECC cusp and greatly underestimates the number of low-energy electrons, even for proton impact.

It is well known [7] that the cusp at $v_e=v$ is ascribed to the Coulomb factor around the projectile

$$|N(\nu_P)|^2=\frac{2\pi\nu_P}{1-\exp(-2\pi\nu_p)}\rightarrow 2\pi\nu_P\rightarrow\infty \text{ as } k_p\rightarrow 0 . \tag{81}$$

The Brinkman-Kramers approximations (BK) contains this factor and thus reproduces the cusp feature. Our BK calculations [Figs. 3(a) and 3(b)] show that this approximation greatly overestimates the cross section, especially for F^{9+}.

The PDSPB approximation also describes both the ECC cusp and the binary peak. Figures 4(a) and 4(b) compare the peaked DSPB theory Eq. (48) with experiment. The PDSPB approximation overestimates the binary-encounter peak, especially for F^{9+}. This is expected since $J\simeq 0$ near the binary-encounter peak and the

peaking approximation Eq. (48) is not valid here.

The DSPB amplitude of Eq. (45) does not require $J \gg Z_T$. Correspondingly, Figs. 5(a) and 5(b), which compare the DSPB cross sections with experiment, reproduce the region from $k_T = v$ to $k_T = 2v$ quite well, especially at the binary-encounter peak. Fainstein, Ponce, and Rivarola [17] obtained results similar to the DPSB curve using the CDW-EIS approximation. The calculations are not directly comparable since Fainstein Ponce, and Rivarola use a different wave function for the He initial state than does the Bates Griffing model employed here. For that reason their DI calculations disagree with experiment even at the binary-encounter peak, while our DI agree with experiment at $k_T = 2v$. Since experiment is normalized at the peak to a binary-encounter calculation the data do not distinguish between the DSPB and CDW-EIS theories.

Because of the uncertainties in the bound-state wave functions for He we compute the cross sections for ion impact on atomic hydrogen targets. Figure 6 compares our DSPB calculations with the DI theory for F^{9+}. We see that the DI and DSPB calculations agree at the binary-encounter peak. Because the binary-encounter peak is used for normalization, we show an expanded view of the binary-encounter region in Fig. 6(b). Note that the present DSPB theory differs from the first Born DI cross section by 8%. The DSPB peak is also shifted to an electron energy slightly below $4(v^2/2)$. This shift appears to agree with experiment in the case of H_2 targets

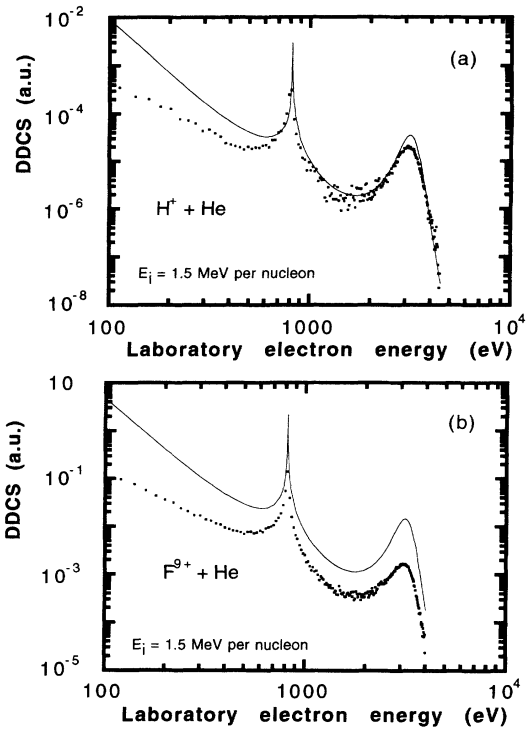

FIG. 3. The double-differential cross section for ejection of electrons of (a) $E_i = 1.5$-MeV protons and (b) 28.5-MeV F^{9+} ions on He atoms. The points are the experimental data of Lee *et al.* [13]. The solid line is the Brinkman-Kramers theory for electron capture to the continuum.

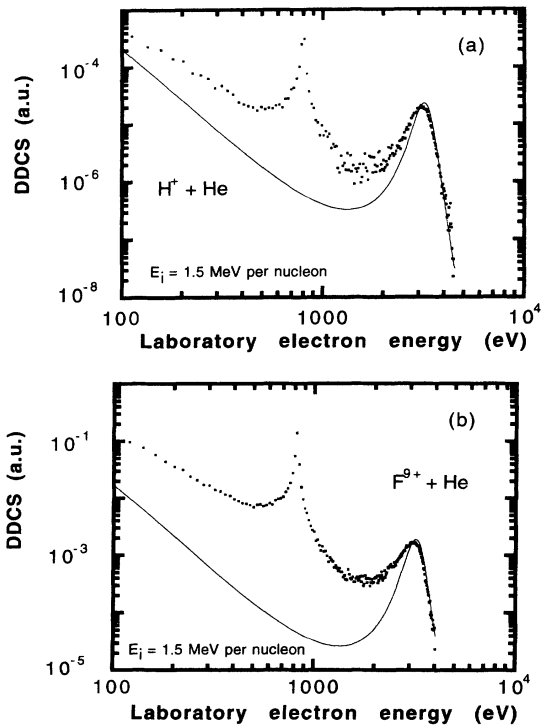

FIG. 2. The double-differential cross section for ejection of electrons of (a) $E_i = 1.5$-MeV protons and (b) 28.5-MeV F^{9+} ions on He atoms. The points are the experimental data of Lee *et al.* [13]. The solid line is the first Born theory for direct ionization.

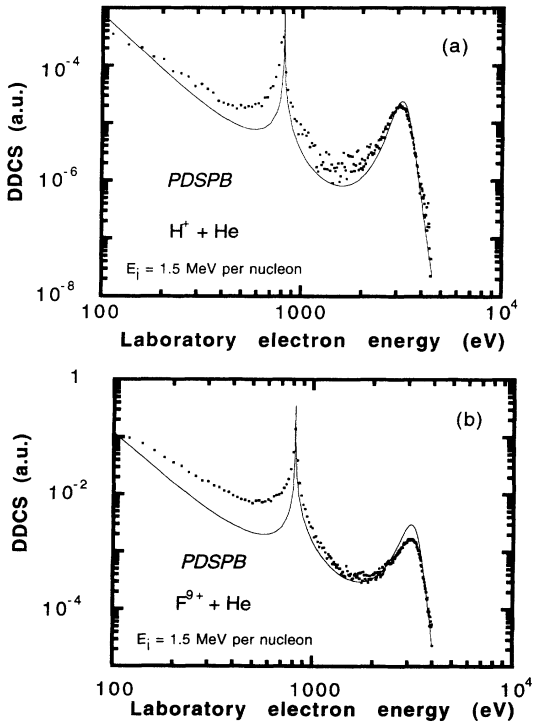

FIG. 4. The double-differential cross section for ejection of electrons of (a) $E_i = 1.5$-MeV protons and (b) 28.5-MeV F^{9+} ions on He atoms. The points are the experimental data of Lee *et al.* [13]. The solid line is the peaked distorted strong-potential Born approximation (PDSPB).

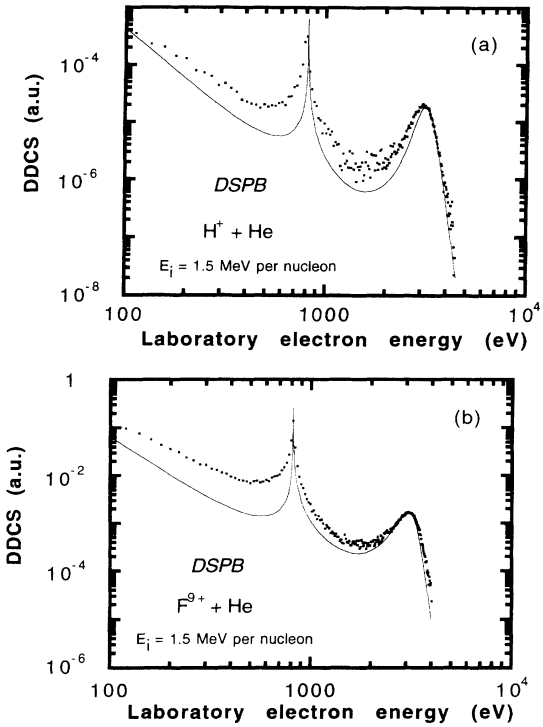

FIG. 5. The double-differential cross section for ejection of electrons of (a) $E_i = 1.5$-MeV protons and (b) 28.5-MeV F^{9+} ions on He atoms. The points are the experimental data of Lee *et al.* [13]. The solid line is the distorted strong-potential Born approximation without peaking (DSPB).

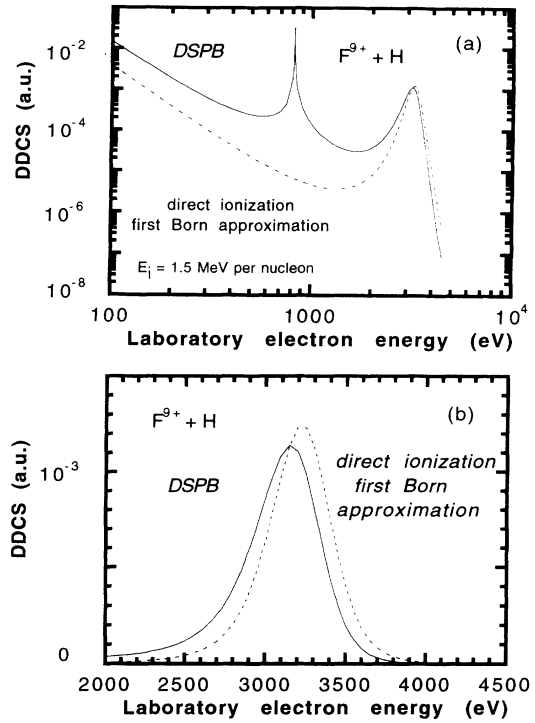

FIG. 6. (a) The double-differential cross section for ejection of electrons of $E_i = 28.5$-MeV F^{9+} ions on H atoms; solid line: the distorted strong-potential Born approximation without peaking (DSPB); broken line: first Born for direct ionization. (b) Same as (a), but only the binary-encounter peak is shown.

[13]. In contrast the calculations of Miraglia and Macek [15] employing a CDW final state and exact evaluation of the integral over s obtain a peak position that is shifted forward of the peak given by the DI theory. Again the calculations are not directly comparable because Ref. (14) considers H_2 targets instead of helium.

None of the theories accurately describe the low-energy electron cross sections. This may indicate an inadequacy of the Bates-Griffing model for these electrons, or it may indicate that two-electron processes play a role.

V. CONCLUSIONS

We have formulated the DSPB theory of impact ionization of atoms by highly charged projectiles. Comparison of computed doubly differential cross sections at 0° with the measurements of Lee *et al.* [13] indicates that the DSPB theory gives a good account of the electron spectra in the region between the binary-encounter peak at electron energies of $4(v^2/2)$ and the continuum capture cusp at $v^2/2$. The cross section for electron energies less than $v^2/2$ lies below experiment by a factor of the order of 4. This discrepancy may be due to our use of the Bates-Griffing model. We therefore show how the Bates-Griffing model derives from the independent-particle approximation. It is possible to employ slightly different independent-particle models which may change the cross sections perhaps giving better agreement with experiment. This is an aspect of the DSPB theory that warrants further investigation.

For H-atom targets the initial-state wave function is known exactly and the independent-electron model is also exact, thus we present calculation for H-atom targets even though experimental data are not available. Comparison of the DSPB theory for H-atom targets with the standard direct ionization theory shows good agreement near the binary-encounter peak, but also indicates that the peak shifts toward lower energy in the DSPB theory.

Finally, a peaked version of the DSPB theory is derived which can be compared with the CDW-CDW theory and the CDW-EIS theory. We find that, in the forward direction, the CDW-CDW and PDSPB amplitudes have almost the same form. The main difference between the two amplitudes is a logarithmic divergence of the CDW-CDW amplitude near the binary-encounter peak which is absent from the PDSPB amplitude. The CDW-EIS amplitude is also similar in form to our PDSPB amplitude, but lacks the Thomas peak. In contrast to the CDW-CDW amplitude, the CDW-EIS amplitude is convergent. CDW-EIS calculations [17] for $F^{9+}+He$ collisions agree with the available data to the same degree as our DSPB calculations. The calculations are not directly comparable owing to the use of different wave functions for the ground state of helium. For that reason we compute the, as-yet-unobserved, cross sections for $F^{9+}+H$. A shift of the binary-encounter peak to an energy below $4(v^2/2)$ is a noteworthy feature of the

DSPB calculations for this system.

ACKNOWLEDGMENTS

We thank Louis J. Dubé for assistance in evaluating the CDW matrix elements. This research was supported by the National Science Foundation under Grant No. PHY-8918713.

APPENDIX A: EVALUATION OF AN INTEGRAL

In this appendix we evaluate the integral over s of Eq. (33) approximately. All of the approximations used are consistent with the peaking approximations [32] used to derive our starting Eq. (30). Together with Eq. (38) one sees that Eq. (33) has the form

$$T^{\mathrm{DSPB}(+)}=-\frac{4\pi Z_T^{5/2}}{(2\pi)^5}N(\nu_P)N(\beta_P) \times \lim_{\lambda_0\to 0}\lim_{\lambda_T\to Z_T}\frac{\partial^2}{\partial\lambda_T\partial\lambda_0}\int_0^1\frac{dt}{\mu^{5/2}}I\ , \tag{A1}$$

with

$$I=\int d\mathbf{s}\,\tilde{\varphi}_i(\mathbf{s},\mu)\frac{C^{a+b-1}}{A^bB^a}{}_2F_1\left[a,b;1;1-\frac{CD}{AB}\right]\ , \tag{A2}$$

$$B(\mathbf{s})=\lambda_0^2-2i\lambda_0|\mathbf{s}-\mathbf{v}_t|+(\mathbf{J}_t+\mathbf{k}_P)^2 -v_t^2-2(\mathbf{K}-\mathbf{k}_P)\cdot\mathbf{s}\ , \tag{A3}$$

$$D(\mathbf{s})=(\lambda_0-ik_P)^2-2(i\lambda_0+k_P)|\mathbf{s}-\mathbf{v}_t| +J_t^2-v_t^2-2\mathbf{K}\cdot\mathbf{s}\ , \tag{A4}$$

$$a=i\nu_P\ , \tag{A5}$$

$$b=i\beta_P\ , \tag{A6}$$

$$\mu^2=(\lambda_T^2+J^2t)(1-t)\ . \tag{A7}$$

Note that we retain the approximation that ν_p is independent of s and t. We rewrite Eq. (A2) with the help of the integral representation

$${}_2F_1(a,b;c;1-z)=\frac{\Gamma(c)}{\Gamma(b)\Gamma(c-b)} \times\int_0^\infty dx\,x^{b-1}(1+x)^{a-c}(1+zx)^{-a} \tag{A8}$$

and use the substitution $y=Cx/A$. We obtain

$$\frac{C^{a+b-1}}{A^aB^a}\,{}_2F_1\left[a,b;1;1-\frac{CD}{AB}\right] =\frac{1}{\Gamma(b)\Gamma(1-b)}\int_0^\infty dy\,y^{b-1}[C+Ay]^{a-1}[B+Dy]^{-a}\ . \tag{A9}$$

This expression is substituted into Eq. (A2) to give

$$I=\frac{1}{\Gamma(b)(1-b)}\int_0^\infty dy\,y^{b-1}[C+Ay]^{a-1}I_1(y)\ , \tag{A10}$$

$$I_1(y)=\int d\mathbf{s}\,\tilde{\varphi}_i(\mathbf{s},\mu)[B(\mathbf{s})+D(\mathbf{s})y]^{-a}\ . \tag{A11}$$

A Taylor-series expansion of $|\mathbf{s}-\mathbf{v}_t|$ for small s gives

$$|\mathbf{s}-\mathbf{v}_t|\simeq v_t-\hat{\mathbf{v}}_t\cdot\mathbf{s} \tag{A12}$$

so that s dependence of $B(\mathbf{s})$ and $D(\mathbf{s})$ is linear,

$$B=B_0+\mathbf{B}_1\cdot\mathbf{s}\ , \tag{A13}$$

$$B_0=\lambda_0^2-2i\lambda_0v_t+(\mathbf{J}_t+\mathbf{k}_P)^2-v_t^2\ , \tag{A14}$$

$$\mathbf{B}_1=2i\lambda_0v_t-2(\mathbf{K}-\mathbf{k}_P)\ , \tag{A15}$$

$$D=D_0+\mathbf{D}_1\cdot\mathbf{s}\ , \tag{A16}$$

$$D_0=(\lambda_0-ik_P)^2-2(i\lambda_0+k_P)v_t+J_t^2-v_t^2\ , \tag{A17}$$

$$\mathbf{D}_1=2(i\lambda_0+k_P)\hat{\mathbf{v}}_t-2\mathbf{K}\ . \tag{A18}$$

Defining

$$\epsilon=2k_P(\hat{\mathbf{v}}_t-\hat{\mathbf{k}}_P) \tag{A19}$$

we may write

$$\mathbf{D}_1=\mathbf{B}_1+\epsilon\ . \tag{A20}$$

We note that ϵ is a small quantity when $k_P\simeq 0$ and when $\hat{\mathbf{v}}_t\simeq\hat{\mathbf{k}}_P$. The integral $I_1(y)$,

$$I_1(y)=\int d\mathbf{s}\,\tilde{\varphi}_1(\mathbf{s},\mu)[(B_0+D_0y)+(\mathbf{B}_1+\mathbf{D}_1y)\cdot\mathbf{s}]^{-a}\ , \tag{A21}$$

is readily evaluated to give

$$I_1(y)=(2\pi)^{3/2}\varphi_{1s}(r_T=0,\mu) \times[(B_0+D_0y)-i\mu|\mathbf{B}_1+\mathbf{D}_1y|]^{-a}\ , \tag{A22}$$

$$I=(2\pi)^{3/2}\varphi_{1s}(r_T=0,\mu)\frac{1}{\Gamma(b)\Gamma(1-b)} \times\int_0^\infty dy\,y^{b-1}[C+Ay]^{a-1} \times[(B_0+D_0y)-i\mu|\mathbf{B}_1+\mathbf{D}_1y|]^{-a}\ . \tag{A23}$$

Our main concern here is to obtain an approximation valid when $J\simeq 0$ where the peaking approximation of Eq. (48) fails. When $J=0$ we have $\mathbf{K}=-\mathbf{v}$ and $k_P\simeq v$ so that $\mathbf{B}_1$ and $\mathbf{D}_1$ are parallel in the limit $\lambda_0\to 0$ and we have

$$|\mathbf{B}_1+\mathbf{D}_1y|=B_1+D_1y\ . \tag{A24}$$

This equation is also valid when ϵ is a small quantity in which case we have

$$|\mathbf{B}_1+\mathbf{D}_1y|\simeq B_1+(B_1+\hat{\mathbf{B}}_1\cdot\epsilon)y\simeq B_1+D_1y \tag{A25}$$

to order ϵ^2. Then we have

$$I=(2\pi)^{3/2}\varphi_{1s}(r_T=0,\mu)\frac{1}{\Gamma(b)\Gamma(1-b)} \times\int_0^\infty dy\,y^{b-1}[C+Ay]^{a-1} \times[(B_0-i\mu B_1)+(D_0-i\mu D_1)y]^{-a}\ . \tag{A26}$$

Because D_1 in Eq. (A26) is multiplied by μ, we see that the error in I due to the approximation (A25) is of order $\mu\epsilon^2$. This is smaller than the errors made in deriving Eq. (30) from Eq. (18). Finally Eq. (A26) together with Eq.

(A9) result in

$$I=(2\pi)^{3/2}\varphi_{1s}(r_T=0,\mu)\frac{C^{a+b-1}}{A^b B^a}\times F_1\left[a,b;1;1-\frac{CD}{AB}\right], \tag{A27}$$

$$B=B_0-i\mu B_1=(\lambda_0-iv_t)^2+(\mathbf{J}_t+\mathbf{k}_p)^2-2i\mu|i\lambda_0\hat{\mathbf{v}}_t+\mathbf{k}_P-\mathbf{K}|, \tag{A28}$$

$$D=D_0-i\mu D_1=D_0-i\mu(B_1+\hat{\mathbf{B}}_1\cdot\boldsymbol{\epsilon})=B-2k_P\left[i\lambda_0+k_P+v_t+\hat{\mathbf{k}}_P\cdot\mathbf{J}_t+i\mu\frac{i\lambda_0\hat{\mathbf{v}}_t+\mathbf{k}_P-\mathbf{K}}{|i\lambda_0\hat{\mathbf{v}}_t+\mathbf{k}_P-\mathbf{K}|}\cdot(\hat{\mathbf{v}}_t-\hat{\mathbf{k}}_P)\right]. \tag{A29}$$

APPENDIX B: THE BATES-GRIFFING MODEL

We consider collisions of projectiles P with targets T. The nucleus charges are Z_P and Z_T and the numbers of electrons are N_P and N_T. The internucleus distance $\mathbf{R}(\mathbf{b},t)$ is a function of the impact parameter $\mathbf{b}$ and the time t. Further $\mathbf{r}_{Pi}$ $(i=1,\ldots,N_P)$ and $\mathbf{r}_{Tk}$ $(k=1,\ldots,N_T)$ are the electron coordinates with respect to the projectile nucleus and the target nucleus, respectively. The U-matrix element for inelastic collisions is

$$U_{fi}=\langle\Phi_f|U|\Phi_i\rangle, \tag{B1}$$

where U is the time evolution operator.

As a first approximation we employ antisymmetrized single-particle wave functions in the singlet state

$$\varphi_i(\mathbf{r}_1,\mathbf{r}_2)=N[\varphi_{1s}(\mathbf{r}_1,Z_{\mathrm{He}})\varphi_{1s}(\mathbf{r}_2,Z_{\mathrm{He}^+})+\varphi_{1s}(\mathbf{r}_2,Z_{\mathrm{He}})\varphi_{1s}(\mathbf{r}_1,Z_{\mathrm{He}^+})]e^{-iE_it}, \tag{B2}$$

$$N=[2+2|\langle\varphi_{1s}(\mathbf{r},Z_{\mathrm{He}})|\varphi_{1s}(\mathbf{r},Z_{\mathrm{He}^+})\rangle|^2]^{-1/2}\simeq\tfrac{1}{2}, \tag{B3}$$

$$\varphi_f(\mathbf{r}_1,\mathbf{r}_2)=\frac{1}{\sqrt{2}}[\varphi_{\mathbf{k}}(\mathbf{r}_1)\varphi_{f2,\mathrm{He}^+}(\mathbf{r}_2)+\varphi_{\mathbf{k}}(\mathbf{r}_2)\varphi_{f1,\mathrm{He}^+}(\mathbf{r}_1)]e^{-iE_ft}. \tag{B4}$$

Here $\varphi_{\mathbf{k}}(\mathbf{r})$ is a Coulomb wave function which describes the ionized electron, and $\varphi_{f,\mathrm{He}^+}(\mathbf{r})$ is a hydrogenic wave function with nuclear charge $Z_{\mathrm{He}^+}=2$ for the He^+ ion. The latter function may represent any final state f. The function $\varphi_{1s}(\mathbf{r},Z)$ is a hydrogenic wave function with nuclear charge Z with the value

$$Z_{\mathrm{He}}=1.345 \tag{B5}$$

or

$$Z_{\mathrm{He}^+}=2.000. \tag{B6}$$

The initial and final energies E_i and E_f are the exact energies of the initial and final states. Using the wave functions (B2)–(B4) and the symmetry of U under electron exchange we have

$$U_{fi}=\left[2\frac{N}{\sqrt{2}}\langle\varphi_{\mathbf{k}}(\mathbf{r}_1)\varphi_{\mathrm{He}^+}(\mathbf{r}_2)|U|\varphi_{1s}(\mathbf{r}_1,Z_{\mathrm{He}})\varphi_{1s}(\mathbf{r}_2,Z_{\mathrm{He}^+})\rangle+2\frac{N}{\sqrt{2}}\langle\varphi_{\mathbf{k}}(\mathbf{r}_1)\varphi_{\mathrm{He}^+}(\mathbf{r}_2)|U|\varphi_{1s}(\mathbf{r}_2,Z_{\mathrm{He}})\varphi_{1s}(\mathbf{r}_1,Z_{\mathrm{He}^+})\rangle\right]\exp[i(E_ft'-E_it)]. \tag{B7}$$

As a second approximation we assume that the operator U is separable (independent-particle approximation)

$$U=U_1U_2 \tag{B8}$$

to write

$$U_{fi}=[\sqrt{2}N\langle\varphi_{\mathbf{k}}(\mathbf{r}_1)|U_1|\varphi_{1s}(\mathbf{r}_1,Z_{\mathrm{He}})\rangle\langle\varphi_{f2,\mathrm{He}^+}(\mathbf{r}_2)|U_2|\varphi_{1s}(\mathbf{r}_2,Z_{\mathrm{He}^+})\rangle+\sqrt{2}N\langle\varphi_{\mathbf{k}}(\mathbf{r}_1)|U_1|\varphi_{1s}(\mathbf{r}_1,Z_{\mathrm{He}^+})\rangle\langle\varphi_{f2,\mathrm{He}^+}(\mathbf{r}_2)|U_2|\varphi_{1s}(\mathbf{r}_2,Z_{\mathrm{He}})\rangle]\exp[i(E_ft'-E_it)]. \tag{B9}$$

With the further approximations

$$\langle\varphi_{\mathbf{k}}(\mathbf{r}_1)|U_1|\varphi_{1s}(\mathbf{r}_1,Z_{\mathrm{He}^+})\rangle\simeq\langle\varphi_{\mathbf{k}}(\mathbf{r}_1)|U_1|\varphi_{1s}(\mathbf{r}_1,Z_{\mathrm{He}})\rangle, \tag{B10}$$

$$\langle\varphi_{f2,\mathrm{He}^+}(\mathbf{r}_2)|U_2|\varphi_{1s}(\mathbf{r}_2,Z_{\mathrm{He}})\rangle\simeq\langle\varphi_{f2,\mathrm{He}^+}(\mathbf{r}_2)|U_2|\varphi_{1s}(\mathbf{r}_2,Z_{\mathrm{He}^+})\rangle,$$

and the definitions

$$E_i=E_{i1}+E_{i2}, \tag{B11}$$

$$E_f=E_{f1}+E_{f2}, \tag{B12}$$

where

$$E_{i2}=-\frac{Z_{\mathrm{He}^+}^2}{2},\quad E_{i1}=E_i-E_{i2}, \tag{B13}$$

$$E_{f2}=-\frac{Z_{\mathrm{He}^+}^2}{2n^2},\quad E_{f1}=\frac{k_P^2}{2}, \tag{B14}$$

and n is the principal quantum number we get the result

$$U_{fi}\simeq 2\sqrt{2}N\langle\varphi_{\mathbf{k}}(\mathbf{r}_1)|U_1|\varphi_{1s}(\mathbf{r}_1,Z_{\mathrm{He}})\rangle\times\exp[i(E_{f1}t'-E_{i1}t)]\times\langle\varphi_{f2,\mathrm{He}^+}(\mathbf{r}_2)|U_2|\varphi_{1s}(\mathbf{r}_2,Z_{\mathrm{He}^+})\rangle\times\exp[i(E_{f2}t'-E_{i2}t)]. \tag{B15}$$

Because of unitarity, the sum over all unobserved final states f_2 of the He^+ ion gives

$$\sum_{f_2}|\langle\varphi_{f_2,\mathrm{He}^+}(\mathbf{r}_2)|U_2|\varphi_{1s}(\mathbf{r}_2,Z_{\mathrm{He}^+})\rangle|^2=1 \tag{B16}$$

so that the probability for emission of one electron independently of the state of the unobserved electron becomes

$$P(\mathbf{b})=\sum_{f_2}|U_{fi}|^2=2|\langle\varphi_{\mathbf{k}}(\mathbf{r}_1)|U_1|\varphi_{1s}(\mathbf{r}_1,Z_{\mathrm{He}})\rangle|^2 . \tag{B17}$$

The factor 2 emerges automatically and represents the fact that the helium atom consists of two electrons. The cross section is given by the integral of $P(\mathbf{b})$ over the impact parameter $\mathbf{b}$,

$$\sigma=\int P(\mathbf{b})d\mathbf{b} . \tag{B18}$$

Following standard arguments we compute the cross section using the time-independent version of the amplitude

$$\langle\varphi_{\mathbf{k}}(\mathbf{r}_1)|U_1|\varphi_{1s}(\mathbf{r}_1,Z_{\mathrm{He}})\rangle\exp[i(E_{f1}t'-E_{i1}t)] .$$

Thus we see that the Bates-Griffing model applies even for highly charged ions.

APPENDIX C: THE CDW-CDW AND CDW-EIS APPROXIMATIONS

In this appendix we examine the divergent behavior of the CDW-CDW T matrix [16]. We set

$$\mathbf{q}=\mathbf{K}_T-\mathbf{K}_i=\mathbf{q}_\perp-\frac{\Delta\varepsilon}{v^2}\mathbf{v} \tag{C1}$$

$$=\mathbf{K}-\mathbf{k}_P , \tag{C2}$$

where $\Delta\varepsilon=E_e-\varepsilon_i$ and E_e and ε_i are the electron energy in the target frame and the binding energy of the (T,e) system, respectively. The transverse component of the momentum transfer is $\mathbf{q}_\perp$ ($\mathbf{q}_\perp\cdot\mathbf{v}=0$). The double-differential cross section is given by

$$\frac{d\sigma}{dE_e d\Omega_e}=k_T\int d\mathbf{q}_\perp|R_{\mathrm{CDW}}(\mathbf{q}_\perp)|^2 , \tag{C3}$$

where we have

$$|R_{\mathrm{CDW}}(\mathbf{q}_\perp)|^2=A(\mathbf{q},\mathbf{k}_T)|N(\nu_T)N(\nu_P)N(\beta_P)|^2|R|^2|{}_2F_1(i\nu_P,i\beta_P;1;z)-i\nu_P\omega_2F_1(1+i\nu_P,1+i\beta_P;2;z)|^2 , \tag{C4}$$

$$\omega=\frac{\alpha}{\gamma}\frac{B\delta+C\gamma}{B(\alpha+\beta)} , \tag{C5}$$

$$A(\mathbf{q},\mathbf{k}_T)=\begin{cases}1 & \text{for } q^2>k_T^2+Z_T^2\\ e^{-2\pi\nu_P} & \text{for } q^2<k_T^2+Z_T^2 ,\end{cases} \tag{C6}$$

$$B=q^2+(1+i\nu_T)\mathbf{q}\cdot\mathbf{k}_T , \tag{C7}$$

$$C=\frac{v}{k_P}[\mathbf{q}\cdot\mathbf{k}_T+k_T^2(1+iv_T)]-\left[1+\frac{v}{k_P}\right][\mathbf{q}\cdot\mathbf{v}+\mathbf{k}_T\cdot\mathbf{v}(1+i\nu_T)] , \tag{C8}$$

$$|R|^2=\frac{2^7}{\pi^2}\frac{Z_P^2Z_T^5}{v^2q^4}\frac{\exp\{-2\nu_T\tan^{-1}[2k_TZ_T/(q^2-k_T^2+Z_T^2)]\}[(q^2+\mathbf{q}\cdot\mathbf{k}_T)^2+(\mathbf{q}\cdot\hat{\mathbf{k}}_T)^2Z_T^2]}{[(\mathbf{k}_T+\mathbf{q})^2+Z_T^2]^4[(q-k_T)^2+Z_T^2][(q+k_T)^2+Z_T^2]} , \tag{C9}$$

$$\alpha=\frac{q^2}{2} , \tag{C10}$$

$$\beta=-\tfrac{1}{2}(k_T^2+Z_T^2) , \tag{C11}$$

$$\gamma=\tfrac{1}{2}[(\mathbf{q}+\mathbf{k}_T)^2+Z_T^2]=\tfrac{1}{2}[J^2+Z_T^2] , \tag{C12}$$

$$\delta=\mathbf{k}_P\cdot\mathbf{v}-k_Pv+\beta , \tag{C13}$$

$$z=\frac{\beta\gamma-\alpha\delta}{\gamma(\alpha+\beta)} . \tag{C14}$$

Note that B and C of this appendix are not related to the parameters B and C used elsewhere in this paper.

In Eq. (C4) the expression for ω and z becomes infinite where $(\alpha+\beta)=0$. We set

$$\omega=\frac{\omega_0}{\alpha+\beta} , \tag{C15}$$

$$z=\frac{z_0}{\alpha+\beta} , \tag{C16}$$

with

$$\alpha+\beta=\tfrac{1}{2}[K^2+k_P^2-2\mathbf{k}_P\cdot\mathbf{K}-k_T^2-Z_T^2]$$
$$=\tfrac{1}{2}[(\mathbf{J}+\mathbf{k}_p)^2-v^2] . \tag{C17}$$

The analytical continuation [33] of the hypergeometric functions

$$ {}_2F_1(a,b;c;z)=\frac{\Gamma(c)\Gamma(b-a)}{\Gamma(b)\Gamma(c-a)}(-z)^{-a}{}_2F_1\left[a,1-c+a;1-b+a;\frac{1}{z}\right] + \frac{\Gamma(c)\Gamma(a-b)}{\Gamma(a)\Gamma(c-b)}(-z)^{-b}{}_2F_1\left[b,1-c+b;1-a+b;\frac{1}{z}\right] \tag{C18} $$

gives

$$ \omega\,{}_2F_1(1+i\nu_P,1+i\beta_P;2;z)=\omega_0\left[(\alpha+\beta)^{i\nu_P}\frac{\Gamma(2)\Gamma(i\beta_P-i\nu_P)}{\Gamma(1+i\beta_P)\Gamma(1-i\nu_P)}(-z_0)^{-i\nu_P-1} \times{}_2F_1\left[1+i\nu_P,i\nu_P;1+i\nu_P-i\beta_P;\frac{\alpha+\beta}{z_0}\right] +(\alpha+\beta)^{i\beta_P}\frac{\Gamma(2)\Gamma(i\nu_P-i\beta_P)}{\Gamma(1+i\nu_P)\Gamma(1-i\beta_P)}(-z_0)^{-i\beta_P-1} \times{}_2F_1\left[1+i\beta_P,i\beta_P;1-i\nu_P+i\beta_P;\frac{\alpha+\beta}{z_0}\right]\right] \tag{C19} $$

provided $z_0\neq 0$. Near $\alpha+\beta=0$ the expression (C19) has a divergent phase and oscillates rapidly in magnitude for $\beta_P\neq\nu_P$.

When

$$ \nu_P=\beta_P \tag{C20} $$

which implies

$$ k_P=|\mathbf{k}_T-\mathbf{v}|=v \tag{C21} $$

we use [33]

$$ {}_2F_1(a,a;c;z)=\frac{\Gamma(c)}{\Gamma(a)\Gamma(c-a)}(-z)^{-a} \times\sum_{n=0}^{\infty}\frac{(a)_n(1-c+a)_n}{(n!)^2}z^{-n}[\ln(-z)+2\psi(n+1)-\psi(a+n)-\psi(c-a-n)] \tag{C22} $$

for $\alpha+\beta\to 0$ and $|z|\to\infty$. Equation (C22) shows that the T matrix diverges logarithmically when $|\mathbf{J}+\mathbf{k}_P|=v$ and $k_P=v$. This occurs near the binary-encounter peak for electron ejection angles greater than $\nu_T/2$.

The CDW-EIS [18] amplitude differs from the CDW-CDW amplitude only in the expression for ω, A, and z,

$$ \omega=\frac{\alpha}{\gamma}\frac{B\delta+C\gamma}{B\beta}\ , \tag{C23} $$

$$ A=e^{-\pi\nu_P}\ , \tag{C24} $$

$$ z=\frac{\beta\gamma-\alpha\delta}{\beta\gamma}\ . \tag{C25} $$

Because β is negative definite ω and z never become infinite.

[1] M. E. Rudd and J. H. Macek, Case Stud. At. Phys. **3**, 47 (1972).
[2] I. A. Sellin, in *Physics of Electron and Atomic Collisions,* edited by S. Datz (Amsterdam, 1982), p. 199.
[3] M. Inokuti, Rev. Mod. Phys. **43**, 297 (1971).
[4] N. F. Mott and H. S. W. Massey, *The Theory of Atomic Collisions* (Oxford University Press, Oxford, 1965).
[5] M. E. Rudd, C. A. Sauter, and C. L. Bailey, Phys. Rev. **151**, 20 (1966).
[6] A. Salin, J. Phys. B **2**, 631 (1969).
[7] J. H. Macek, Phys. Rev. A **1**, 235 (1970).
[8] K. Dettman, K. G. Harrison, and M. W. Lucas, J. Phys. B **7**, 269 (1974).
[9] J. S. Briggs, J. Phys. B **10**, 3075 (1977).
[10] J. H. Macek, J. Phys. B **18**, L71 (1985); Phys. Rev. A **37**, 2365 (1988); J. Phys. B **24**, 5121 (1991).
[11] D. P. Dewangan and J. Eichler, J. Phys. B **18**, L65 (1985).
[12] K. Taulbjerg, R. O. Barrachina, and J. H. Macek, Phys. Rev. A **41**, 207 (1990).
[13] D. H. Lee, P. Richard, T. J. Zouros, J. M. Sanders, J. L. Shinpaugh, and H. Hidmi, Phys. Rev. A **41**, 4816 (1991).
[14] D. H. Jakubassa-Amundsen, J. Phys. B **16**, 1767 (1983).

[15] J. E. Miraglia and J. H. Macek, Phys. Rev. A **43**, 5919 (1991).
[16] Dz. Belkic, J. Phys. B **11**, 3529 (1978).
[17] P. D. Fainstein, V. H. Ponce, and R. D. Rivarola, J. Phys. B **24**, 3091 (1991).
[18] D. S. F. Crothers and J. F. McCann, J. Phys. B **16**, 3229 (1983).
[19] R. Shakeshaft, Phys. Rev. A **17**, 1011 (1978).
[20] D. H. Jakubassa-Amundsen and P. A. Amundsen, Z. Phys. A **297**, 203 (1980).
[21] J. H. Macek and S. Alston, Phys. Rev. A **26**, 250 (1982).
[22] N. C. Deb, N. C. Sil, and J. H. McGuire, J. Math. Phys. **26**, 2670 (1986).
[23] H. Marxer and J. S. Briggs, Z. Phys. D **13**, 75 (1989).
[24] D. R. Bates and G. Griffing, Proc. Phys. Soc. London, Sect. A **66**, 961 (1953).
[25] R. P. Feynman, Phys. Rev. **76**, 769 (1949).
[26] S. D. Oh, J. H. Macek, and E. Kelsey, Phys. Rev. A **17**, 873 (1978).
[27] M. L. Goldberger and K. M. Watson, *Collision Theory* (Wiley, New York, 1964).
[28] L. D. Landau and E. M. Lifschitz, *Quantum Mechanics: Non-Relativistic Theory* (Pergamon, London, 1965).
[29] C. O. Reinhold and J. E. Miraglia, J. Phys. B **20**, 1069 (1987).
[30] M. R. H. Rudge, J. Phys. B **2**, 130 (1968).
[31] L. H. Thomas, Proc. R. Soc. London **114**, 501 (1927).
[32] J. S. Briggs and J. H. Macek, Adv. At. Mol. Opt. Phys. **28**, 1 (1991).
[33] *Handbook of Mathematical Functions,* edited by M. Abramowitz and I. A. Stegun (Dover, New York, 1965).